

# Supporting Information

Tang et al. 10.1073/pnas.0906979106

## SI Text

**Single-Molecule FRET Measurements.** All measurements were done at 21 °C–23 °C in 15 mM Tris acetate (pH 7.5), 50 mM sodium acetate, 10 mM magnesium acetate, 5 mM DTT, 0.1 mg/mL BSA, and an oxygen-scavenging system ≈1.5 mM Trolox (Sigma–Aldrich), 0.5% (wt/wt) β-D-glucose, 165 units/mL glucose oxidase, and 2,170 units/mL catalase. Concentration of T7 RNAP, GTP/3' dGTP, and each of the rest of the NTPs used was 10 nM, 1 mM, and 500 μM, respectively.

Double-stranded DNA fragments containing the T7 RNAP class III promoter sequence from –21 to +6 (Table S1) were surface-immobilized via a biotinylated strand B annealed to its 5' tail. Donor fluorophore Cy3 was attached to position –4 in the nontemplate (NT) strand and acceptor fluorophore Cy5 to position +17 in the template (T) strand. Nonspecific binding of RNAP was minimized by using sample cells coated with a mixture of PEG and ≈2% biotinylated PEG (Nektar Therapeutics) (1). Single DNA–RNAP complexes were imaged by wide-field TIR microscopy using a 532-nm diode laser (CrystaLaser) for Cy3 excitation (2). Images were acquired with 30-ms time resolution by using an electron-multiplying CCD camera (iXon DV 887-BI; Andor Technology) and custom C++ routines. Cy3 and Cy5 fluorescence from the sample was split and imaged side by side on the CCD camera. Apparent donor,  $I_D$ , and acceptor,  $I_A$ , signals were estimated by removing donor leakage to acceptor channel (12.5%) and acceptor leakage to donor signal (2%) as well as background. The FRET efficiency,  $E$ , was calculated by using the Eq. S1,

$$E = \left[ 1 + \gamma \frac{I_D}{I_A} \right]^{-1} \quad [\text{S1}]$$

where  $\gamma$  is the ratio of change in average acceptor intensity ( $\Delta I_A$ ) to change in average donor intensity ( $\Delta I_D$ ) before and after acceptor photobleaching. The most probable  $\gamma$  factor was calculated from 25 molecules after their acceptors underwent photobleaching for each stalled position of the T7 RNA polymerase–DNA complex.

**Steady-State FRET Measurements.** Equilibrium FRET measurements were carried out at 25 °C on a FluoroMax-2 spectrofluorometer (Jobin Yvon–Spex Instruments). The reaction buffer was 50 mM Tris acetate (pH 7.5) plus 50 mM sodium acetate, 10 mM magnesium acetate, and 1 mM fresh DTT. FRET efficiencies ( $E_{\text{FRET}}$ ) of T7 RNAP transcription were calculated by (ratio)<sub>A</sub> method (3, 4).

**Stopped-Flow FRET Measurements.** Real-time measurements of donor and acceptor fluorescence intensities were carried out on a T-scheme KinTek stopped-flow setup (Mode 2001) after rapid mixing of nucleotide substrates from one syringe with the preincubated T7 RNAP (150 nM) and doubly dye-labeled

promoter DNA (100 nM; TAMRA as the donor and A647 as acceptor) from a second other syringe (all concentrations were final). The final concentrations of nucleotides were 1 mM for GTP or 3' dGTP, and 0.4 mM for each of all of the other NTPs or 3' dNTPs. The fluorescence intensity of TAMRA was measured by using a 580-nm band-pass filter ( $\pm 5$ nm), and that of A647 was measured by using a 630-nm long-pass filter. Fluorescence signals at each translocated position of transcription were averaged from 8–10 shots. The time courses of fluorescence were fitted to the following exponential equation (Eq. S2), and the goodness of fitting was as justified by visible inspection and by the random distribution of residuals.

$$F_{(t)} = F_0 + \sum \Delta F_i \exp(-k_i t) \quad (i = 1, 2 \text{ or } 3) \quad [\text{S2}]$$

FRET efficiency was determined from the change of donor fluorescence in the presence of acceptor according to Eq. S3:

$$E = 1 - \frac{F_{DA}}{F_D} \quad [\text{S3}]$$

where  $F_D$  and  $F_{DA}$  are the fluorescence intensities of donor in the absence and presence of acceptor, respectively. FRET in the preformed binary complex,  $E_{RP}$ , is contributed by both the closed and open complexes and is equal to  $1 - F_D^{RP}/F_D$ . The observed fluorescence intensities of the donor at time  $t$  of the transcription reaction,  $F_{D(t)}^{TC}$ , are related to the FRET efficiency,  $E_{(t)}$ , by the following Eq. S4.

$$E_t = 1 - \frac{F_{D(t)}^{TC}}{F_D} \quad [\text{S4}]$$

At the start of the experiment ( $t = 0$ ), it is the fluorescence intensity of the preformed polymerase–promoter complex (RP),  $F_{RP}$ , that contributes to FRET, rather than  $F_D$  ( $F_0 = F_{RP}$ ). The two values are related accordingly. Thus, Eq. S4 was modified to the following:

$$E_t = 1 - \frac{F_{D(t)}^{TC}}{F_{RP}}(1 - E_{RP}) = 1 - \frac{F_{D(t)}^{TC}}{F_{D(0)}}(1 - E_{RP}) \quad [\text{S5}]$$

**Transient-State Kinetics of RNA Polymerization.** T7 RNAP (15 μM final) and promoter DNA (10 μM final) were preincubated in the transcription buffer [50 mM Tris acetate (pH 7.5), 100 mM sodium acetate, 10 mM magnesium acetate, and 5 mM DTT], and 20 μL was mixed with an equal volume of the four rNTPs (1 mM each) spiked with [ $\gamma$ - $^{32}$ P]GTP for designated time intervals before stopping the reactions with 200 mM EDTA (pH 8.0). RNA products were resolved on a 23% polyacrylamide/4 M urea sequencing gel and were visualized/analyzed by phosphorimaging using Typhoon 9410 and ImageQuant (Molecular Dynamics).

1. Rasnik I, Myong S, Cheng W, Lohman TM, Ha T (2004) DNA-binding orientation and domain conformation of the *E. coli* rep helicase monomer bound to a partial duplex junction: Single-molecule studies of fluorescently labeled enzymes. *J Mol Biol* 336:395–408.  
2. Roy R, Hohng S, Ha T (2008) A practical guide to single-molecule FRET. *Nature Methods* 5:507–516.

3. Tang G-Q, Patel SS (2006) T7 RNA polymerase-induced bending of promoter DNA is coupled to DNA opening. *Biochemistry* 45:4936–4946.  
4. Clegg RM, et al. (1992) Fluorescence resonance energy transfer analysis of the structure of the four-way DNA junction. *Biochemistry* 31:4846–4856.

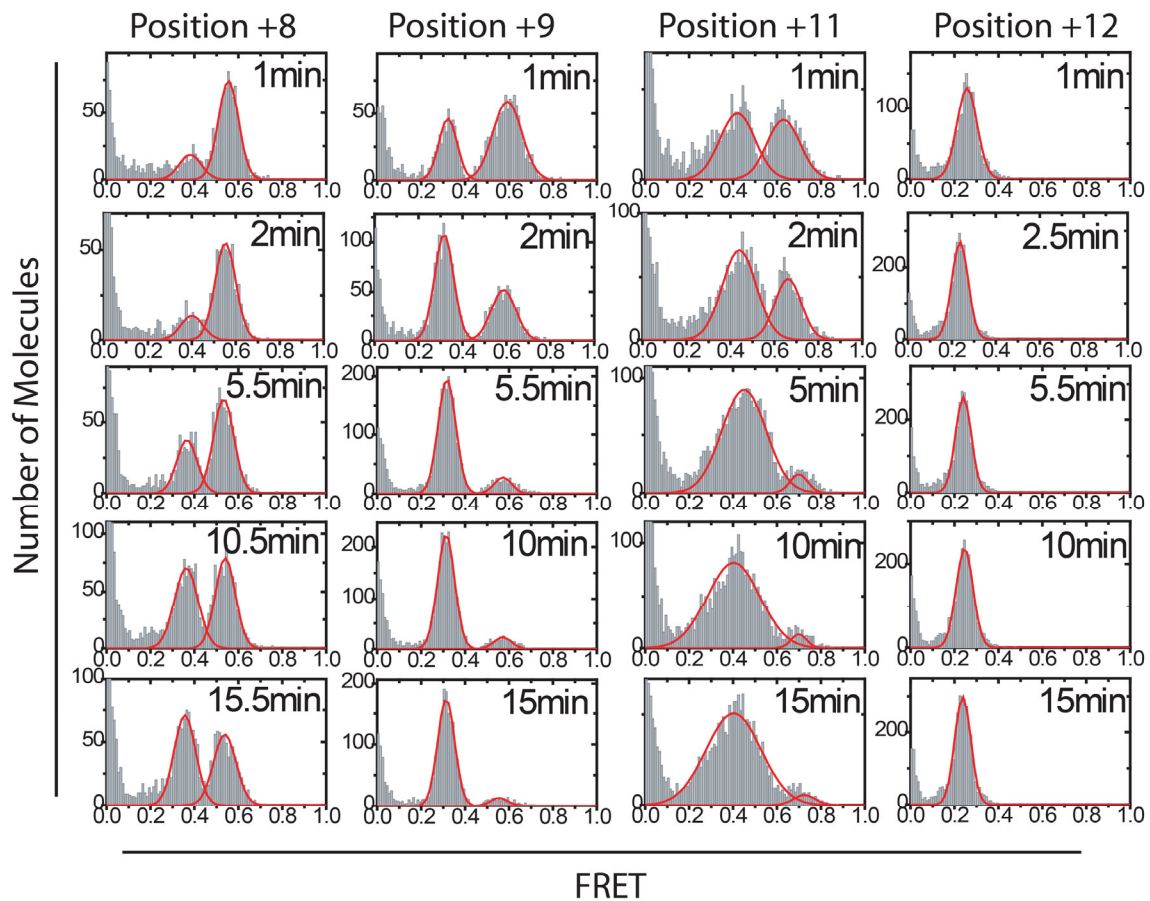


**Fig. S1.** Kinetics of IC-to-EC transition measured by single-molecule FRET. Time-dependent changes in FRET distribution of T7 RNAP-transcribing complexes halted at positions at +8, +9, +11, and +12. Measuring conditions were the same as described in Fig. S2. The x axis of the histograms denotes corrected FRET, and y axis denotes the number of molecules. Data for +8, +9, and +11 were fitted to two Gaussian distributions (smoothed curves), and data for +12 were fitted to a single distribution. The high-FRET IC population slowly converts to a low-FRET EC population. At +12, only EC (FRET  $\approx 0.25$ ) was present all of the time of observation.

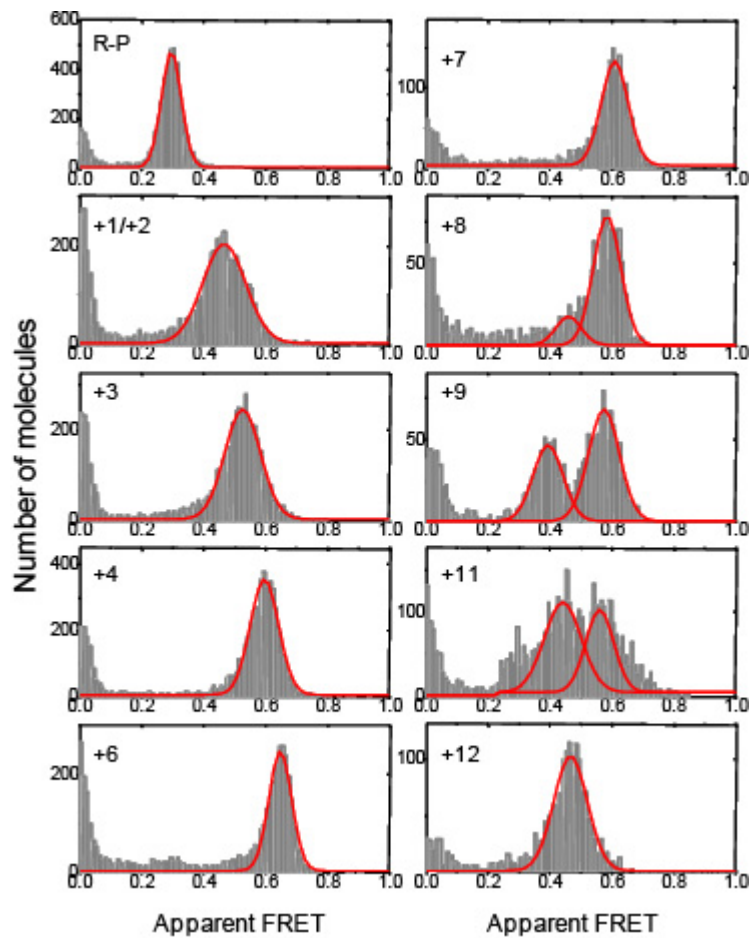
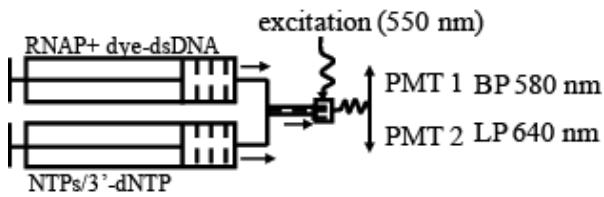


**Fig. S2.** FRET histograms. The x axis shows apparent single-molecule FRET efficiency,  $E_{app}$ . [ $E_{app(infi)} = I_A / (I_D + I_A)$ , without  $\gamma$ -function correction], and the y axis shows observed numbers of transcribing molecules. T7 RNAP transcription was halted at designed positions under limiting NTPs with or without 3' dNTP.



A



B

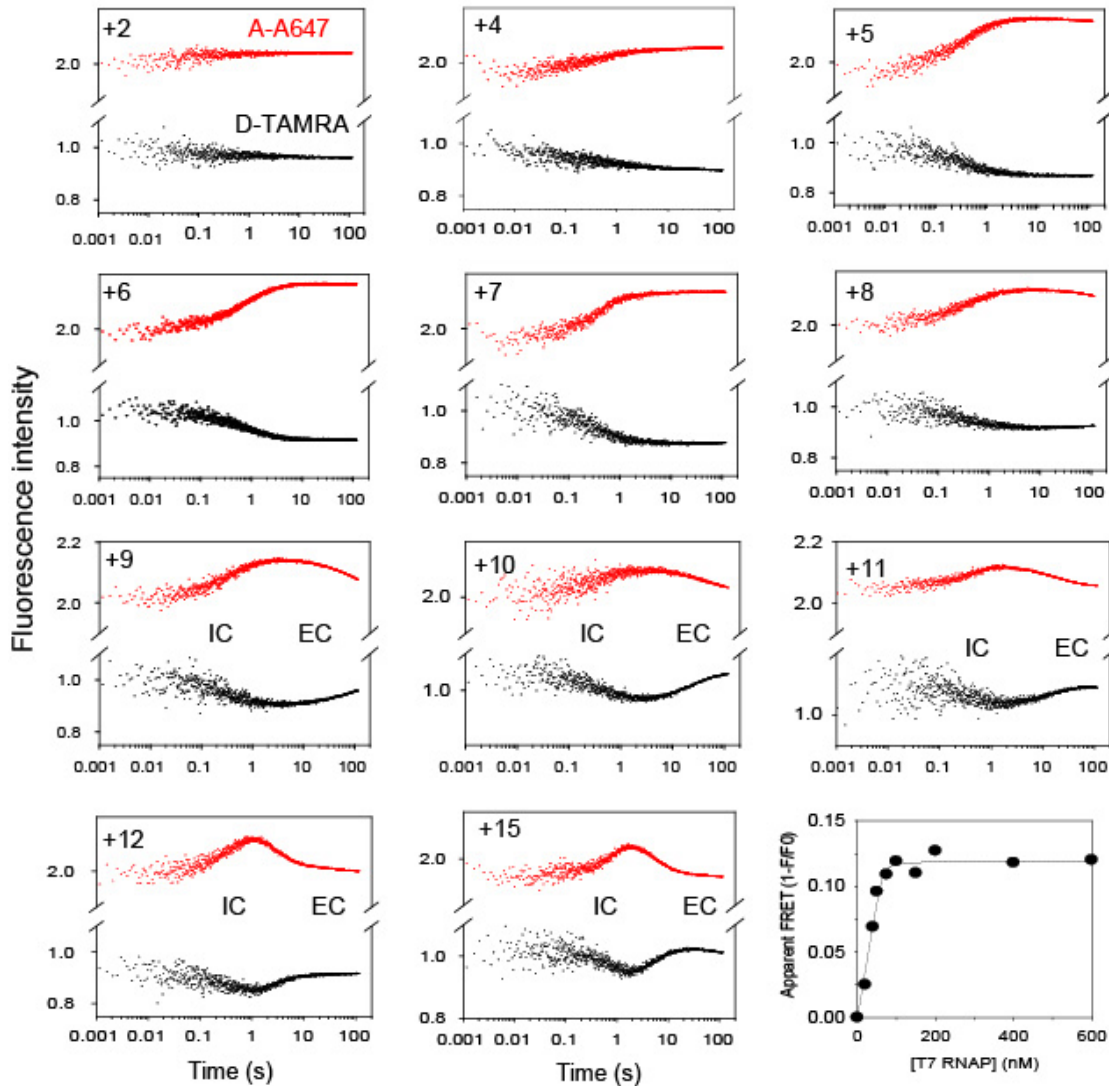


**Fig. S4.** T7 RNAP transcription measured by stopped-flow FRET. (A) A schematic stopped-flow FRET assay of transcription. A preformed mixture of 150 nM RNAP and 100 nM doubly labeled duplex promoter (TAMRA-5'-NT/A647-5'-T; both are final concentrations) (Eqs. s1, s3, s5, or s8) in one syringe of the KinTek stopped-flow setup was rapidly mixed with limiting nucleotides (1 mM GTP or 3' dGTP, 0.4 mM for each of the other NTPs or 3' dNTP, final) at 25 °C. Excitation was set on 550 nm. The donor signal was observed through a 580-nm centered band-pass filter ( $\pm 5$ nm) and the acceptor signal through a 640-nm long-pass filter, both in a log time scale. (B) Real-time traces of the donor (black, lower trace in each graph) and acceptor (red, upper trace in each graph) fluorescence intensities as T7 RNAP transcription was halted on positions indicated. The last graph shows stopped-flow FRET titration of T7 RNAP and promoter DNA in transcription up to +6 by increasing T7 RNAP concentrations in mixtures of 50 nM dye doubly labeled DNA and constant GTP and ATP, yielding  $K_d = 0.8$  nM for the +6 halted transcribing complex. This indicated that the transcribing complex with an increase in RNA/DNA hybrid length became less stable compared with the initial open complex formed with 3' dGTP.



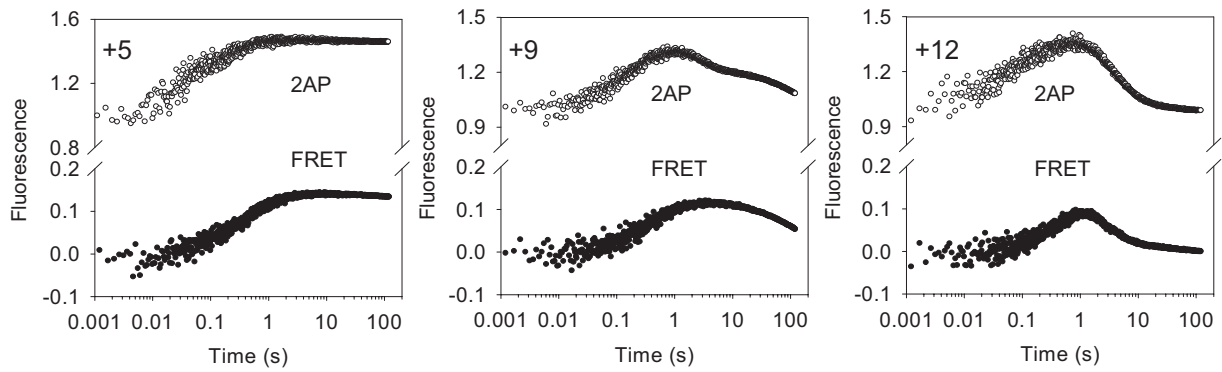


**Fig. S6.** Kinetics of initial bubble reclosure and promoter bending/unbending. Stopped-flow kinetic traces of transcription reactions on the consensus promoter halted on +5, +9, and +12 monitored by 2AP (at  $-4T$ ) fluorescence changes (upper traces) or FRET (acceptor fluorescence; lower traces) changes. To facilitate comparison, FRET data were modified by using  $I_A/I_{A0} - 1$ , where  $I_A$  and  $I_{A0}$  were acceptor intensities at times  $t$  and 0, respectively.

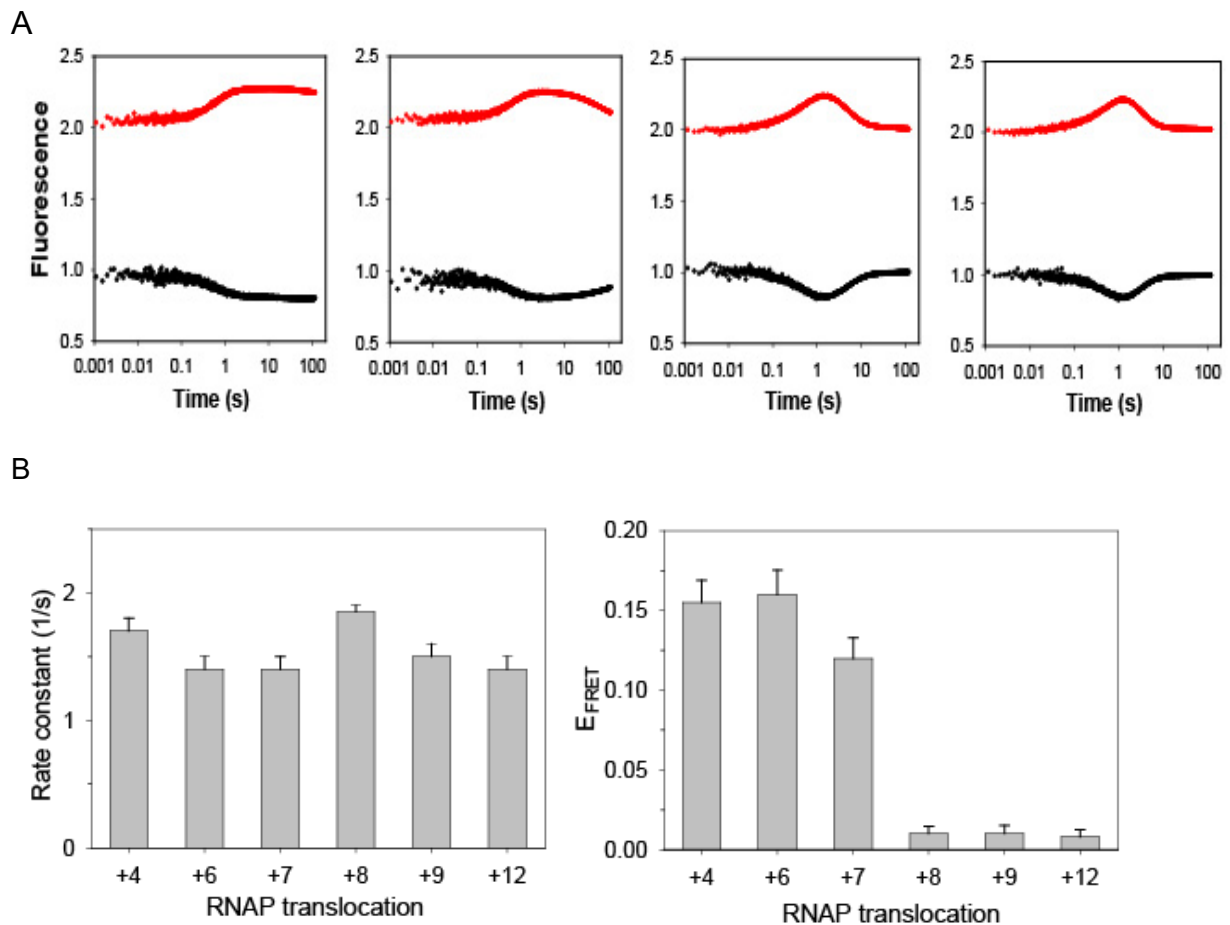


**Fig. S7.** Early IC-to-EC transition in the A-15C mutant promoter. (A) Stopped-flow traces showing donor and acceptor fluorescence changes in A-15C promoter in reactions halted at the indicated positions. Late-phase FRET decrease, and hence IC-to-EC transition, occurs earlier, starting at +7 in the A-15C promoter. (B) Rate constant of early-phase FRET increase with the A-15C promoter in reactions halted at the positions indicated (*Left*). FRET efficiency at 120 s after the transcription was initiated with the A-15C promoter and halted at various indicated positions (*Right*). FRET values were determined from donor quenching according to Eqs. S2–S5. Error bars show the range of data from two measurements.

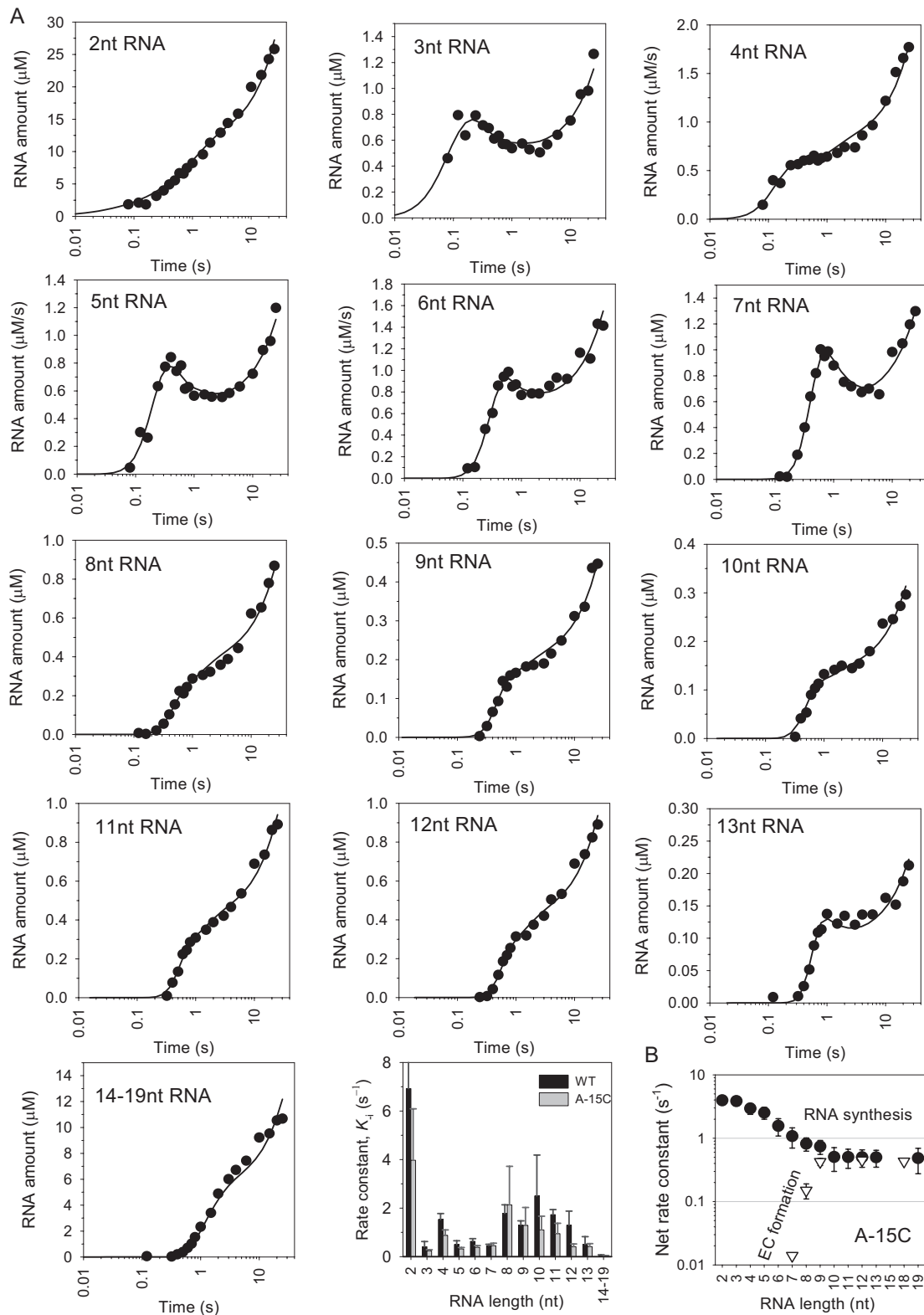


**Fig. 58.** Kinetic analysis of the transcription initiation pathway. (A) The time course of formation and decay of individual RNAs (2, 6, 8, 12, and 19 nt) from data in Fig. 5A. The time courses were globally fit to the transcription model in Fig. 5B by using the Global Kinetic Explorer program (KinTek). The elementary rate constants of nucleotide addition are shown in Fig. 5C, and the last panel shows the elementary dissociation rate constants of 2- to 19-nt RNA from the transcribing complex of the consensus promoter (black bars) and the A-15C promoter variant (gray bars). (B) The net rate constants of RNA syntheses of different lengths (filled circles) and the net rate constants of EC formation (blank triangles) at these translocation steps for the A-15C promoter variant. Error bars represent the range of data from two or more measurements.

